

PAPER • OPEN ACCESS

Simulation and research on fracture behavior of vehicle structural alloy materials based on XFEM

To cite this article: Peiyuan Li *et al* 2023 *J. Phys.: Conf. Ser.* **2512** 012002

View the [article online](#) for updates and enhancements.

You may also like

- [Micromechanical finite element analysis of effect of multilayer interphase on crack propagation in SiC/SiC composites](#)
Fang Guangwu, Sun Jie, Gao Xiguang et al.
- [A review of extended/generalized finite element methods for material modeling](#)
Ted Belytschko, Robert Gracie and Giulio Ventura
- [Numerical analysis of the mechanical and electrical properties of \(RE\)BCO tapes with multiple edge cracks](#)
Jintao Ma and Yuanwen Gao



ECS
The
Electrochemical
Society
Advancing solid state &
electrochemical science & technology

DISCOVER
how sustainability
intersects with
electrochemistry & solid
state science research

Simulation and research on fracture behavior of vehicle structural alloy materials based on XFEM

Peiyuan Li, Qiaoyan Cai *, Fei Wang, Tao Zhang

China Academy of Launch Vehicle Technology. No.1 Nandahongmen Rd. Beijing, CHINA

Caiqy2019@163.com

Li_py@foxmail.com

Abstract. Aluminum alloy 7050 has been widely used in the structure of aerospace vehicles because of its excellent comprehensive performance. In this paper, based on the extended finite element method and classical theory, the material parameters in the finite element simulation are calculated, next the metal plate with a central pre-crack is analyzed for static load breaking and fatigue damage under cyclic loading, the observation of different loading levels and the damage characteristics under different preset crack lengths are summarized, the rules are summarized to provide support for follow-up work.

1. Introduction

Aluminium alloy 7050 is widely used in aerospace structures due to good performance and machinability, it is also used as structural material in reusable aerospace vehicles. Unlike aircraft, the vehicle has a wide flight space, heavy loads on the structure, and low requirements for flight life, generally belong to the category of low cycle fatigue. Therefore, when evaluating its structural life, the emphasis is on damage tolerance analysis.

In 1999, Beleytachko and others in the United States proposed the Extended Finite Element Method (XFEM)^[1]. In the calculation process, the description of the discontinuity field is completely independent of the grid boundary, so it is widely used to deal with discontinuity problems such as cracks, voids, and interface layers. Compared with the traditional finite element method, the mesh used by this method has nothing to do with the geometry or physical interface inside the structure, thus overcoming the difficulties brought about by high-density meshing in areas of high stress and deformation concentration such as crack tips. When simulating the crack growth path, there is no need to re-mesh, which greatly reduces the calculation cost.



K Rege and H G Lemu^[2] present methods and recent developments in simulating fatigue crack growth using the FEM and XFEM method. B Trollé et al.^[3] studies XFEM crack growth under rolling contact fatigue. Gairola S and Jayaganthan R^[4] simulated the behavior of tensile fracture inside the alloy, and calculated the stress intensity factor and J integral in different working conditions. And learned that when analyzing fracture toughness problems, the simulation results of the 3D finite element model are better. Bashir R et al.^[5] combined the Von Mises criterion to analyze the stress field near the mode I crack tip and predict the crack propagation direction. Nur Azam Abdullah et al.^[6] and R Rashnooie et al.^[7] evaluated the intralaminar and interlaminar damage of composite laminates and the damage behavior of composite-metal bonding surfaces and predicted fatigue life based on the XFEM method. C Duan et al.^[8] studied the fracture behavior of turbine alloy materials at different temperatures, calculated the stress intensity factor at the tip of crack in different temperatures, the extended finite element crack length is solved to obtain the fatigue crack growth rate da/dN curve. Wickramasinghe et al.^[9] studied the crack propagation behavior of rails under compressive vibration.

2. Calculation of Material Fracture Parameters

Abaqus allows users to add different keywords to select different fracture criteria. In the research problem of low cycle fatigue crack using the power law as the fracture criterion, keywords in the following format need to be added^[10]: *fracture criterion, type=fatigue, mixed mode behavior=power. In the finite element analysis of fatigue crack growth based on ABAQUS, the fatigue crack growth initiation criterion is defined as^[10]:

$$f = \frac{N}{c_1 \Delta G^{c_2}} \geq 1.0 \quad (1)$$

The relationship between the crack growth rate and ΔG is:

$$\frac{da}{dN} = c_3 \Delta G^{c_4} \quad (2)$$

ΔG is the relative fracture energy release rate when the structure is loaded between its maximum and minimum values.

According to the Paris' law^[11], the functional relationship between the crack growth rate and the difference between the maximum and minimum values of the stress intensity factor K is:

$$\frac{da}{dN} = c \Delta K^m \quad (3)$$

Considering that in the category of linear elastic fracture mechanics, there is the following relationship between the strain energy release rate G and the stress intensity factor K ^[12]

$$G = \frac{K^2}{E'} \quad (4)$$

$$\Delta G = \frac{(\Delta K)^2}{E'} \quad (5)$$

So it can be deduced that:

$$\frac{da}{dN} = c_3 \left[\frac{(\Delta K)^2}{E'} \right]^{c_4} = c_3 \left(\frac{1}{E'} \right)^{c_4} (\Delta K)^{2c_4} \quad (6)$$

In the formula,

$$\text{(Plane Stress)} \quad (7)$$

$$E' = \begin{cases} E=69000 \text{ MPa} \\ \frac{E}{1-\mu^2}=77432 \text{ MPa} \end{cases} \quad (\text{Plane Strain})$$

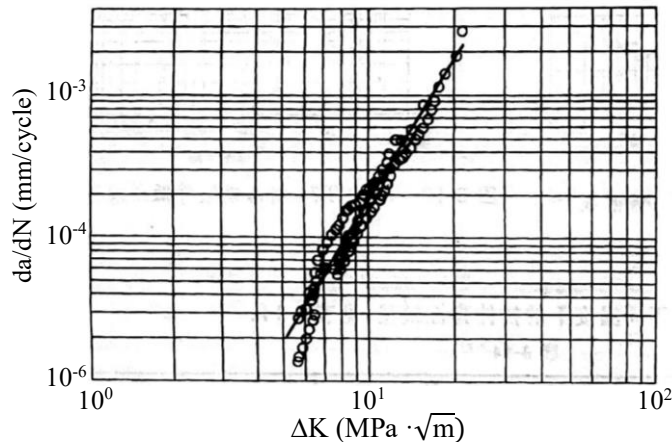


Figure 1. Crack growth rate curve of aluminum alloy 7050.

According to the data^[13], the Paris' law formula for crack growth of aluminum alloy 7050 plate is:

$$\frac{da}{dN} = 9.601732 \times 10^{-8} (\Delta K)^{3.2627} \quad (\text{mm/cycle}) / (\text{MPa} \cdot \sqrt{\text{m}}) \quad (8)$$

Consequently:

$$c_3 = C(E')^{c_4} = 1.22546 \times 10^{-12} \times 77432^{1.63135} = 1.15835 \times 10^{-4} \quad (9)$$

$$c_4 = \frac{m}{2} = 1.63135 \quad (10)$$

$$\frac{da}{dN} = c_3 \Delta G^{c_4} = 1.15835 \times 10^{-4} \Delta G^{1.63135} \quad (\text{mm/cycle}) / (\text{MPa} \cdot \text{mm}) \quad (11)$$

The power law model given below is described by Wu and Reuter^[14], the low-cycle fatigue onset and crack growth criterion for mixed mode behavior as type Power Law.

$$\frac{G_{\text{equiv}}}{G_{\text{equivC}}} = \left(\frac{G_I}{G_{IC}} \right)^{a_m} + \left(\frac{G_{II}}{G_{IIC}} \right)^{a_n} + \left(\frac{G_{III}}{G_{IIIC}} \right)^{a_o} \quad (12)$$

In the formula, G_{equiv} is the equivalent strain energy release rate, G_{equivC} is the critical equivalent strain energy release rate, G_I , G_{II} , and G_{III} are the strain energy release rates corresponding to type I, type II, and type III cracks, respectively, and G_{IC} , G_{IIC} , and G_{IIIC} are respectively The critical strain energy release rate corresponding to type I, II and III cracks.

Integrate the " σ - ε " curve to calculate its fracture energy, the calculated material parameters are shown in table 1:

$$W = d \int_0^{\varepsilon_0} \sigma d\varepsilon \quad (13)$$

Table 1. Material fracture performance parameters.

c_1^a	c_2^a	c_3^a	c_4^a	$\frac{G_{\text{thresh}}^b}{G_C}$	$\frac{G_{\text{pl}}^c}{G_C}$
0.5	-0.1	1.1584×10^{-4}	1.6314	0.01	0.85
G_{IC}^d	G_{IIC}^d	G_{IIIC}^d	a_m^e	a_n^e	a_o^e
10.12	10.12	10.12	1	1	1

^a Material constant for fatigue crack initiation/growth, $(\text{mm} \cdot \text{cycle}^{-1}) \cdot (\text{MPa} \cdot \text{mm})^{-0.5}$.

^b Ratio of energy release rate threshold used in the Paris law over the equivalent critical energy release rate, the default value is 0.1, when the value is lower than this value, the crack will not expand.

^c Ratio of energy release rate upper limit used in the Paris law over the equivalent critical energy release rate, the default value is 0.85, the crack growth is significantly accelerated above this value.

^d Mode I/ II III critical energy release rate, $\text{MPa} \cdot \text{mm}$.

^e Exponent, the default value is 1.

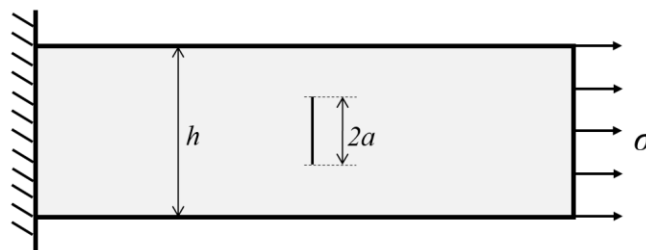


Figure 2. Plate with pre-cracks subjected to plane tension.

As shown in the figure 2, it is a flat plate with a finite width of h , there is a penetrating straight crack with a length of $2a$ in the middle, the two ends away from the crack are subjected to uniform unidirectional tensile stress σ , which can be known from the knowledge of linear elastic fracture mechanics, the calculation formula of the stress intensity factor including the correction factor is^[12]:

$$K_I = Y\sigma\sqrt{\pi a} \tag{14}$$

In the formula,

$$Y = \frac{1}{\sqrt{\pi}} \left[1.77 + 0.227 \left(\frac{a}{h} \right) - 0.51 \left(\frac{a}{h} \right)^2 + 2.7 \left(\frac{a}{h} \right)^3 \right] \tag{15}$$

When $\sigma=400\text{MPa}$, $a=3\text{mm}$, $h=100\text{mm}$, $Y=1.0025$, the K_I value is shown in the table 2:

Table 2. Comparison of theoretical and simulated values of stress intensity factor.

Theoretical Value K_I ($\text{MPa} \cdot \sqrt{\text{mm}}$)	FEM Calculation Value of K_I ($\text{MPa} \cdot \sqrt{\text{mm}}$)	Relative Error %
1230.7	1243	0.996

After comparison, the relative error of the finite element software calculation results compared with the theoretical value is 0.996%, which is within the allowable error range. Therefore, the finite element modeling in this example is scientific and effective, so it can be used for subsequent calculation and analysis.

3. Simulation and Analysis of Fracture of Plate with Pre-cracks

The relationship between crack growth and loading of 7050 aluminum alloy plate with pre-cracks was studied in the process of quasi-static tension. A plate with a width of 100 mm is fixed at one end and a

displacement is applied at the free end. Place a crack which initial width is 4mm in the center of the plate and allow it to grow in the static analysis step. Analysis step length is 1.0. Using fracture energy as the basis for crack growth, the elements type adopts C3D8R.

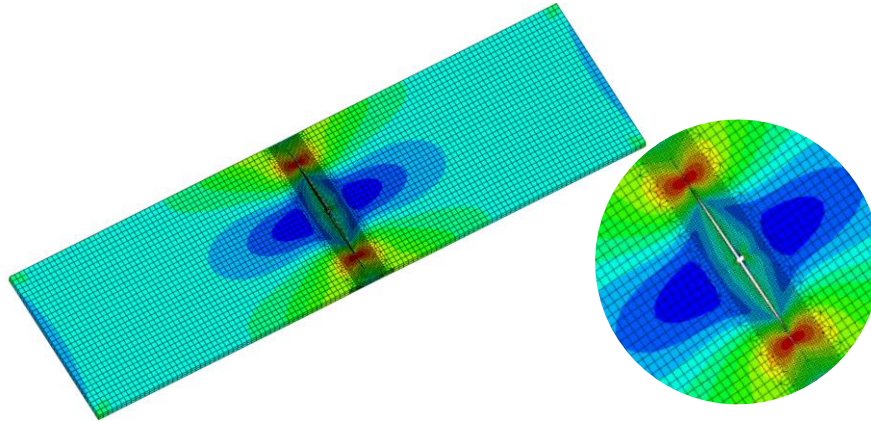


Figure 3. Crack propagation and stress distribution at the crack tip.

When a preset crack with a fixed length of 4mm is arranged in the center of the plate, the free end is loaded with displacements of different lengths, the change of crack length expansion with step time is shown in the figure 4. As can be seen from the figure, although the free end is loaded with displacements of different lengths and levels, the loading displacements of free edge when cracks start to propagate in the plate under different loading conditions are roughly the same, about 1.1 mm, when the displacement loading length is about 2.4 mm, all the plates are damaged. At the same time, it can be observed that when the crack length reaches about 8 mm, the propagation speed becomes significantly faster, after entering the accelerated cracking stage, the crack of plate with a larger loading displacement level will grow faster and the slope of the curve will be larger, this means that the structure will suddenly break down at this time. The internal stress of the plate with a smaller displacement loading level is smaller, it may not enter the stage of accelerated crack growth from the beginning to the end.

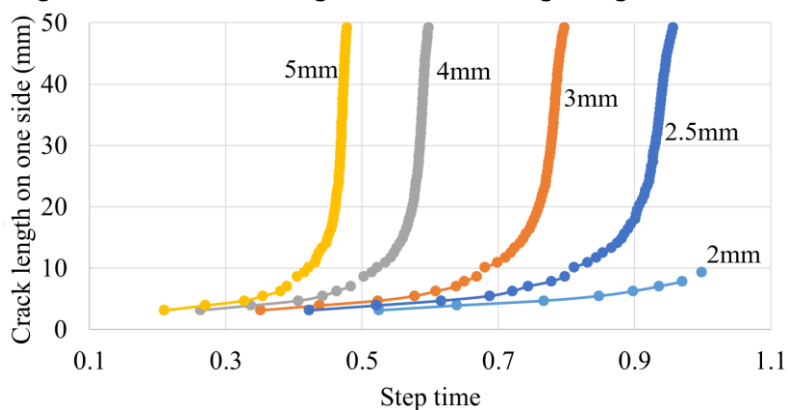


Figure 4. Growth of crack length when loaded with different load displacements.

When pre-set cracks of different lengths are arranged in the center of the plate, a fixed displacement of 3 mm is loaded at the free end, figure 5 shows the variation of crack length growth with step time. As can be seen from the figure, although the initial lengths of cracks are at different levels, the final aluminum alloy panels are all damaged under the same displacement loading level. This is due to the difference in crack growth rate. In general, the shorter the initial length of the crack, the slower the crack growth rate in the slow crack growth stage, and the larger the proportion of time in the crack slow growth

stage; the longer the initial crack length, the faster it will enter into the crack significant in the expansion stage. At the end of the length of the crack growth, the growth rate becomes slow due to the geometric deformation of the structure, since the displacement is applied at the midpoint of the free end of the plate, when the crack propagates to the edge of the plate, the tensile displacement at the crack tip is much smaller than that at the center point of the plate.

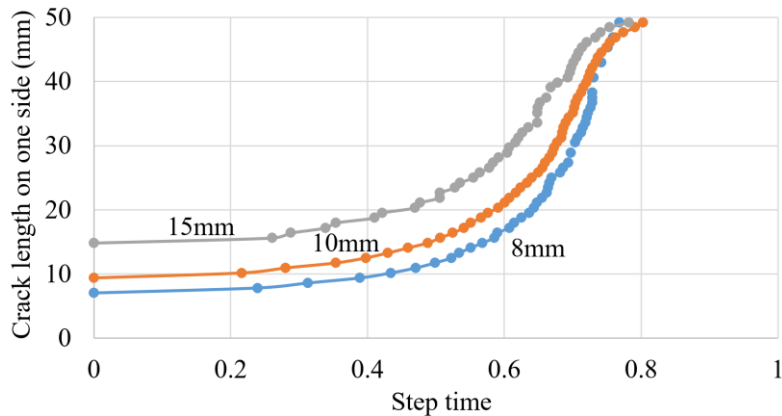


Figure 5. Crack growth length of pre-cracks of different lengths as a function of loading.

Aiming at the preset crack with a length of 6 mm in the center of the plate, different tensile displacements of $R=0.1$ are cyclically applied to the free end of the plate, and the fatigue life within 1 million cycles of loading under different working conditions is calculated. As shown in the figure 6, the crack length of the plate varies with the number of cycles when the maximum tensile displacement is 0.2 mm, 0.3 mm, 0.5 mm and 0.8 mm. It can be seen from the figure that when the crack extends to about 9mm, the rate of crack propagation becomes significantly faster, the plate is completely destroyed in a short time. The smaller the level of loading displacement, the longer the period of crack growth rate acceleration. The number of cycles corresponding to when the crack starts to grow and the plate is completely destroyed is shown in the table 3:

Table 3. The number of cycles corresponding to the crack propagation and complete failure of the plate under different loading levels.

Load (mm)	The number of cycles corresponding to the initial crack growth	The number of cycles corresponding to the plate is completely damaged
0.2	144390	Not completely failure
0.3	23258	129730
0.5	5712	52500
0.8	1584	5534

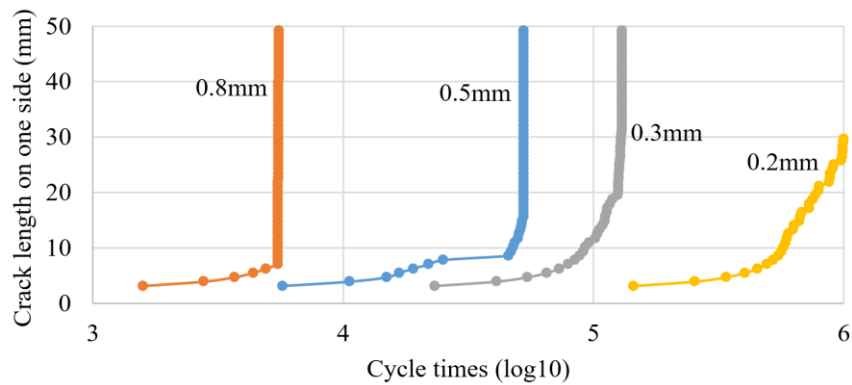


Figure 6. Relationship between crack length and cycle times under different cyclic loading levels.

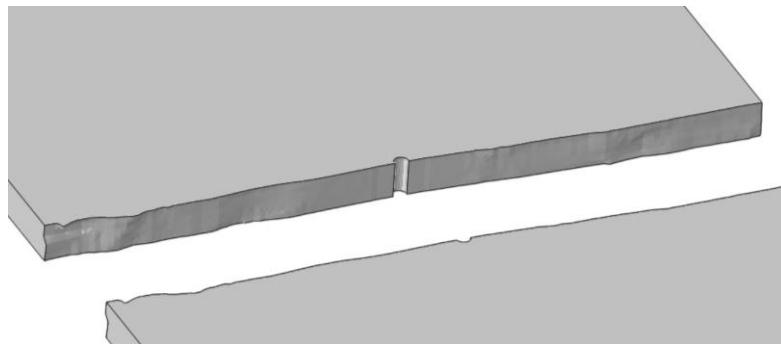


Figure7. Figure a fatigue fracture surface.

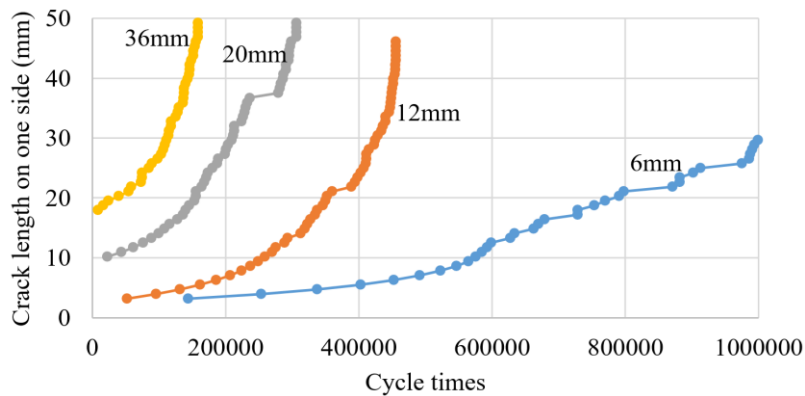


Figure 8. Variation of crack propagation in plates with different lengths of preset cracks.

When pre-cracks of different lengths are arranged in the middle of the plate, it can be seen that the longer the pre-crack length, the shorter the fatigue life and the greater the growth rate in the crack rapid growth stage. When the preset crack length is greater than the threshold of significant expansion, the crack enters the stage of rapid expansion. It can also be inferred that if the initial crack length is less than the threshold value, the crack will not enter the stage of significant growth.

Next, the evolution law of the pre-crack length at the side of one lug hole of the vehicle with different loading levels will be explored. There is a preset crack with a length of 1 mm on the side of the connecting hole of the lug. With different levels of tensile displacement loading, the evolution of the crack length is shown in figure 9, the stress field at the crack tip and fracture surface are shown in figure 10. It can be seen that although some discrete data points appear due to randomness, the overall law is

consistent with the previous research content.

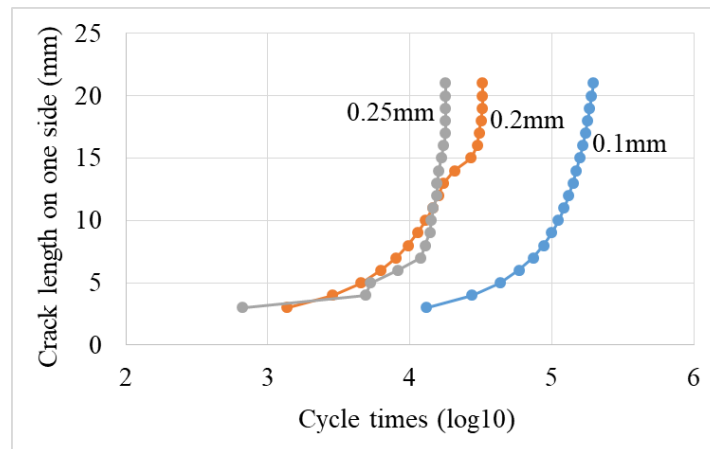


Figure 9. The growth of the crack length at the side of the lug hole

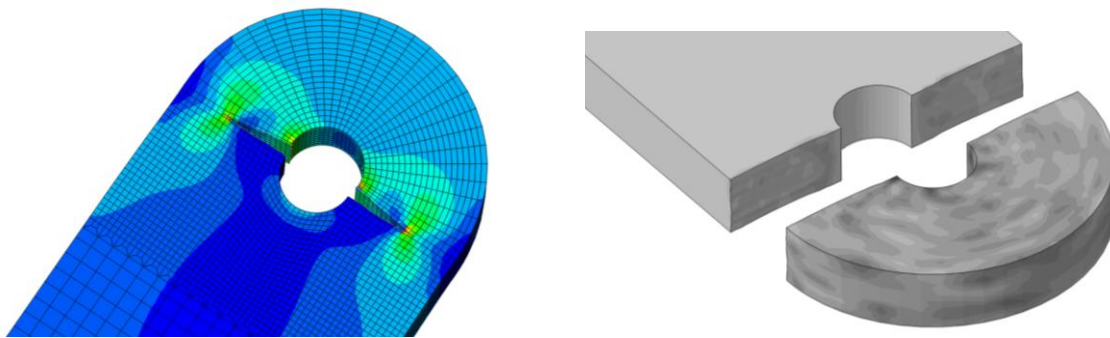


Figure 10. The typical stress field at the crack tip and the fracture surface.

4. Conclusion

Through the above analysis, we can calculate the material parameters when the finite element analysis software performs fracture simulation through the intrinsic parameters of the material. Through the finite element simulation analysis, it can be seen that the metal plate with pre-cracks is more sensitive to the influence of load changes. When the crack growth length exceeds the threshold, the crack will accelerate the expansion, causing the structure to be destroyed instantaneously. Control the load level of structure within a certain range, the fatigue damage will never occur in service life control the crack length below the threshold value, it will not cause the structure to break suddenly. The plastic parameters of the material can be further introduced later, more accurate results can be obtained as a guide for actual engineering.

5. References

- [1] Moes N, Dolbow J and Belytschko T 1999 A Finite Element Method for Crack Growth without Remeshing *International Journal for Numerical Methods in Engineering* 46. 131-150 10.1002/(SICI)1097-0207(19990910)46:13.0.CO;2-J.
- [2] Rege K and Lemu H 2017 A review of fatigue crack propagation modelling techniques using FEM and XFEM. *IOP Conf. Series Materials Science and Engineering* 276. 012027. 10.1088/1757-899X/276/1/012027.

- [3] Trollé B, Baietto M, Gravouil A, Mai S and Nguyen-Tajan T 2013 XFEM Crack Propagation Under Rolling Contact Fatigue *Procedia Engineering* **66** 775-782 <https://doi.org/10.1016/j.proeng.2013.12.131>.
- [4] Gairola S and Ren J 2021 XFEM Simulation of Tensile and Fracture Behavior of Ultrafine-Grained Al 6061 Alloy. *Metals*. **11**. 1761. 10.3390/met11111761.
- [5] Bashir R, He X, Usman M, Irshad M, and Hayat N 2021 Prediction of the Direction of XFEM Crack Based on Von Mises Around the Crack-tip under Mode-I 10.20944/Preprints202106.0261.v1.
- [6] Abdullah N, Curiel-Sosa, J, Taylor Z, Tafazzolimoghaddam B, Vicente, J and Zhang C 2017. Transversal crack and delamination of laminates using XFEM *Composite Structures*. **173** p78-85. 10.1016/j.compstruct.2017.04.011.
- [7] Rashnooie R, Zeinoddini M, Ahmadpour F, Beheshti Aval S and Chen T 2022 A coupled XFEM fatigue modelling of crack growth, delamination and bridging in FRP strengthened metallic plates *Engineering Fracture Mechanics* <https://doi.org/10.1016/j.engfracmech.2022.109017>.
- [8] Duan C, Chen X and Li R 2020 The numerical simulation of fatigue crack propagation in Inconel 718 alloy at different temperatures. *Aerospace Systems* 10.1007/s42401-020-00044-z.
- [9] Wickramasinghe I, Hargreaves D, and De Pellegrin D 2013 Predicting crack initiation due to ratchetting in rail heads using critical element analysis *International Journal of Materials Science and Engineering*. **77** p850-856.
- [10] Dassault Systèmes 2014 *ABAQUS user's manual in Ver. 6.14 User's Guide* p Section 10.7.1.
- [11] Paris P and Erdogan F 1963 A critical analysis of crack propagation laws *Journal of Basic Engineering* **85** (4) 528-533 doi:10.1115/1.3656900.
- [12] Li Z and Zhang J 2012 *Engineering Fracture Mechanics*(Chinese) (Beijing: Beijing University of Aeronautics and Astronautics Press).
- [13] Editorial Committee of China Aeronautical Materials Handbook 2002 *China Aeronautical Materials Handbook* (Chinese) Vol. **3** (Beijing: China Standard Press) p306.
- [14] Wu E and Reuter R 1965 Crack Extension in Fiberglass Reinforced Plastics *T and M Report* Vol. **275** (Chicago: University of Illinois).